Int. J. Heat Mass Transfer. Vol. 24, No. 7, pp. 1247–1255, 1981
Printed in Great Britain

0017–9310/81/071247–09 $02.00/0
Pergamon Press Ltd.

HEAT TRANSFER FROM RAREFIED IONIZED ARGON GAS TO A BIASED TUNGSTEN FINE WIRE

TAKUYA HONDA, TAKASHI HAYASHI† and ATSUSHI KANZAWA
Department of Chemical Engineering, Tokyo Institute of Technology, Meguroku, Tokyo, Japan

(*Received* 27 *May* 1980)

Abstract — Experimental and theoretical studies have been made of heat transfer from a rarefied, partially ionized argon plasma jet (500 Pa, 9000 K) to a biased tungsten fine wire.

The heat flow rates to the wire were obtained from its electrical resistance variations. When the wire is biased, the resistance cannot be measured accurately because the current through the bias circuit obstructs the measurements. Therefore, the current was broken by a switching circuit for a short time (0.1 ms) every 3 ms to measure the resistance.

The variation of heat flow rates with a biased potential could be obtained, and the accommodation coefficients of argon atoms and ions were determined, resulting in 0.62 for argon atoms and 0.48 for argon ions.

NOMENCLATURE

a_j, thermal accommodation coefficient of species j;
E_j, energy of type j [J];
e, unit charge [C];
f_j, Maxwell–Boltzmann velocity distribution function of species j;
i_j, current of species j [A m^{-2}];
i_s, saturation ion current [A m^{-2}];
k, Boltzmann constant [J K^{-1}];
l, length of a probe [m];
m_j, mass of species j [kg];
n_j, number density of species j [m^{-3}];
$\mathbf{P}$, position vector [m];
P, pressure [Pa];
Q_j, heat flow due to species j per unit length [W m^{-1}];
q, total heat flux [W m^{-2}];
q_j, heat flux due to species j [W m^{-2}];
$q_{0.99}$, heat flux at the break time which is one hundredth of T_s [W m^{-2}];
R, radius of the probe [m];
r, radial coordinate of plasma jet [mm];
T, thermal equilibrium temperature [K];
T_b, break time of square wave potential [s];
T_j, temperature of species j [K];
T_s, period of square wave potential [s];
T_w, temperature of wall [K];
$\mathbf{u}_0$, flow velocity vector [m s^{-1}];
u_I, ionization potential [J];
u_0, flow velocity [m s^{-1}];
V_j, first-order mean velocity of species j [m s^{-1}];
v, peculiar velocity [m s^{-1}];
v', volume element [m^3];
w, particle velocity [m s^{-1}];
y, u_0/V;
z, axial coordinate of plasma jet [mm].

Greek symbols

α', angle defined by Fig. 10;
β_j, species js correction factor due to the effect of flow velocity on q_k;
γ_j, species j's correction factor due to the effect of flow velocity on q_i;
θ, ϕ, ψ, angles defined by Fig. 10;
τ, time [s];
ϕ, probe potential with respect to the plasma potential [V];
ϕ_w, work function [V].

Superscripts

*, critical.

Subscripts

F, float condition;
i, ionization energy;
k, kinetic energy;
p, electric potential;
s, sheath;
1, argon atoms;
2, argon ions;
3, electrons.

1. INTRODUCTION

RAREFIED ionized gas heat transfer problems are of great interest in the fields of plasma chemistry, low pressure discharge technology, etc. Rarefied gas heat transfer has other aspects in comparison with continuum one; i.e. it depends mainly on the accommodation coefficient and pressure.

There have been many studies concerning the heat

†Present address: Mitsui Sekiyu Kagaku Co.

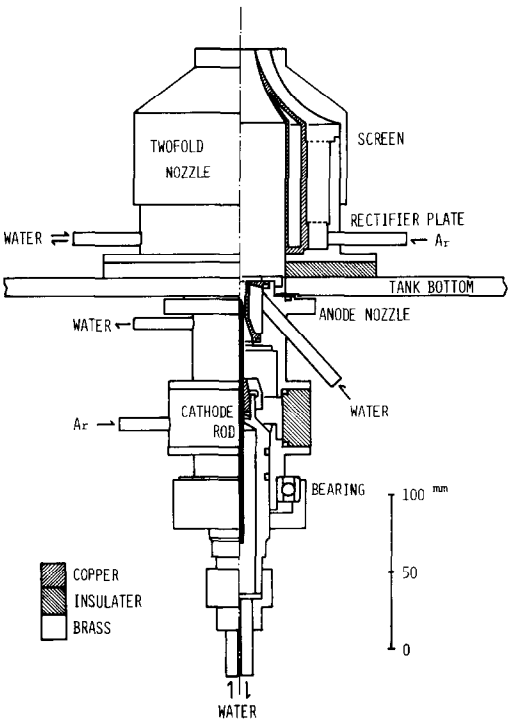

FIG. 1. Twofold nozzle and plasma jet generator.

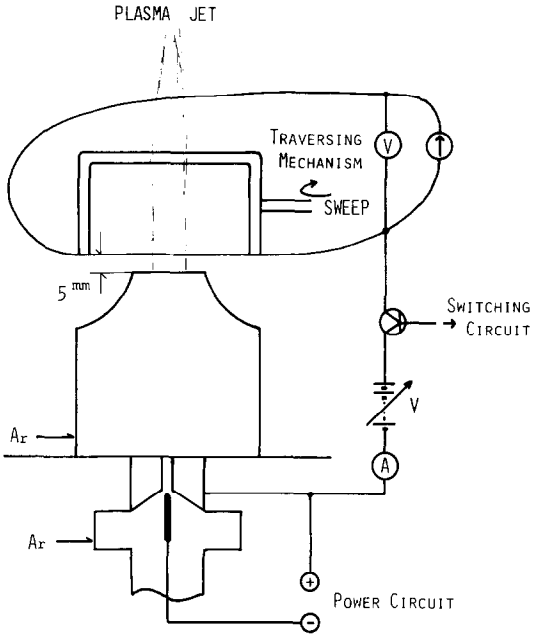

FIG. 2. Probe and electric circuit arrangement.

transfer from a non-ionized rarefied gas to a solid surface [1–3] and the accommodation coefficients for the several combinations between a non-ionized gas and a solid wall. These are summarized by Devienne [4] and Springer [5]. However, there have been few studies for a high temperature range, including ionization phenomena, and few values of the accommodation coefficients have been obtained.

Ionized gas heat transfer is affected by an electric or magnetic field, and by the recombination of ions and electrons on the surface, because of the presence of ionized species. In this study, firstly, the effects of an electric field on the heat transfer were investigated by using a biased fine tungsten wire and plasma jet; both of which are considered to be the best devices for this type of application. The heat transfer to the wire can be measured from the electric resistance variations of the wire. In this case, an ion and/or electron currents (probe current) flow into the wire because of the potential difference. These currents and its resistance variations must be measured simultaneously, so a pulse circuit was developed to break and connect the bias circuit alternatively. The biased potential used in this experiment ranged from -30 to -3 V.

Secondly, electron temperature was evaluated from the measurements of the probe current; namely, the wire works as an electrostatic probe, i.e. a Langmuir probe, as well as a calorimetric probe.

Thirdly, the accommodation coefficients of argon atoms and ions were estimated from the comparison with the measured and theoretical heat flux variations with a probe potential.

2. EXPERIMENTS

2.1. *Experimental apparatus*

Figure 1 shows the twofold nozzle and plasma jet generator. These are fixed at the bottom of the vacuum tank whose diameter and height are 0.5 and 1.5 m, respectively. The D.C. plasma jet generator is constructed of an 8 mm I.D. copper anode nozzle and a 6 mm dia. tungsten cathode rod. The plasma jet is generated by the arc discharge under the conditions of 22–28 V and 120–130 A. Both of the electrodes were cooled by water to protect from thermal damage. The anode and tank were electrically earthed.

The twofold nozzle was constructed of a 20 mm I.D. copper inner and 40 mm I.D. brass outer. The inner is cooled by water, and both of them were electrically floated from the plasma jet. The plasma jet was ejected upward through the inner, and the external coaxial argon gas flow was ejected through the gap between the inner and outer to stabilize the jet.

The flow rate of the argon plasma jet was 0.11 g s^{-1}, and that of the coaxial argon gas flow was 0.25 g s^{-1}. The argon gas was allowed to flow for $\frac{1}{2}$ h prior to, and $\frac{1}{2}$–1 h following, ignition to displace the residual gas and to stabilize the arc. The pressure of the tank was kept at 500 Pa with the argon gas flow under these conditions.

The jet axis and radius are denoted by z and r, respectively, with the origin at the center of the exit plane of the plasma jet nozzle.

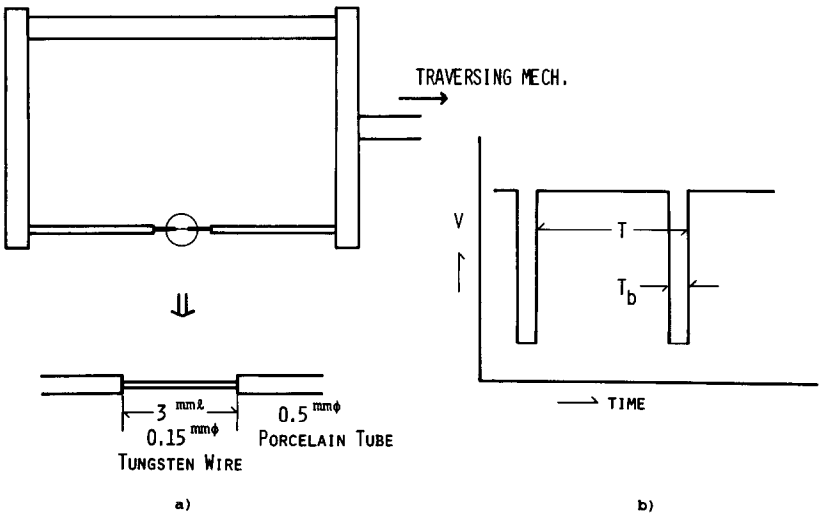

FIG. 3. (a) Probe. (b) Schematic illustration of a square wave potential; the high level indicates the bias circuit is connected, and the low indicates the circuit is broken.

2.2. *Measurements*

Heat flow from the plasma jet, saturation ion current and electron temperature were simultaneously measured by a wire probe. The probe was traversed in the plane perpendicular to the jet to protect it from thermal damage, and the plane was 5 mm above the plasma jet exit (Fig. 2).

The variation of the electric resistance of the probe was measured to obtain the heat flow to the biased probe. As an ion and/or electron current flows into the probe during the heat flow measurement, these currents cause an electric potential drop along the wire of the probe, and obstruct the accurate measurement of the heat flow. Therefore, it is necessary to break the biased potential at the moment of the heat flow measurement.

The probe was constructed of a 0.15 mm dia., 3 mm long tungsten wire and 0.5 mm O.D. porcelain tubes to support the wire as shown in Fig. 3(a).

In this experiment, the square wave potential as shown in Fig. 3(b) was applied to the probe through an electric switching circuit described below. T_s denotes the period and is usually fixed at 3 ms (*ca.* 330 Hz). T_b is the break time and variable, but it was fixed at one thirtieth of T_s, 0.1 ms, in this experiment for a reason that will be described later. During the remaining time,

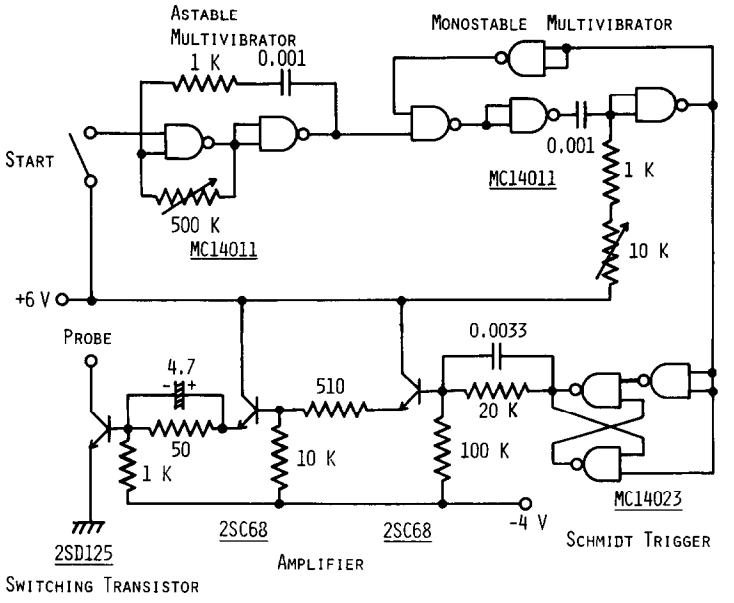

FIG. 4. Electric circuit generating square waves and switching transistor.

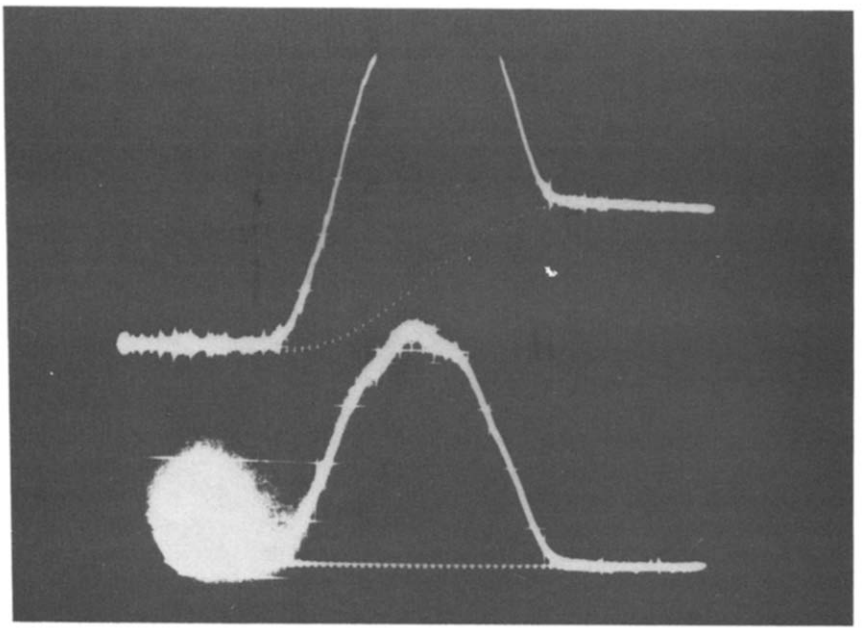

FIG. 5. A typical photograph of CRT measuring a heat flow and probe current.

2.9 ms, an arbitrary potential ($-30 \sim -3$ V) was applied to the probe.

The electric resistance variation of the probe was measured at the time interval T_b every 3.0 ms to obtain the heat flow. On the other hand, at the rest of the time intervals, $T_s - T_b$, an arbitrary electric potential was applied to the probe and the probe current was measured. So, the heat flow from the plasma jet to the biased probe and the relationship between the probe current and potential can be obtained simultaneously by using the square wavelike varying potential.

The electric circuit for applying a square wave potential is shown in detail in Fig. 4. An astable multivibrator was used as an oscillator. The square wavelike potential was vibrated at around 330 Hz. The rising heads of potential waves allowed the following monostable multivibrator to be unstable during the time interval determined by the time constant given by R and C, and to be stable after that. The controlling square waves which are 0 V for 0.1–0.2 ms and then +6 V for 3.0 ms (its frequency is around 330 Hz) are generated. These waves are refined by the Schmidt trigger circuit. These waves work a switching transistor, which breaks and connects alternatively the main circuit where a probe current of around 1 A flows.

A typical photograph observed by a synchroscope is shown in Fig. 5. The curves indicate the variation of the probe electric resistance (upper dotted one), that of the probe current (lower solid one), and that of the probe potential drop (upper solid one). The heat flow rate is obtained from the incline of the resistance variation curve. The difference between upper dotted and solid curves is the potential drop along the wire caused by the probe current.

The probe characteristics (the probe current–potential relation) was obtained from the lower solid curve and voltmeter. At the strongly negative potential region, the probe current was constant, and a saturation ion current i_s

$$i_s = \tfrac{1}{4} e n_2 \left(\frac{8kT_2}{\pi m_2} \right)^{1/2} \tag{1}$$

was obtained. If the state of the plasma is at thermal equilibrium; i.e. T_2 and T_1 are equal to T_3 and these are equal to thermal equilibrium temperature T, the density of ions is a function of only T, and thereby i_s is also a function of T. Therefore, the thermal equilibrium temperature T is obtained from equation (1).

On the other hand, at the slightly negative potential region ($i_3 \gg i_2$), the probe current i is written as

$$\ln i = \frac{e\phi}{kT_3} + \text{const.} \tag{2}$$

where ϕ is the potential between the probe and plasma.

3. EXPERIMENTAL RESULTS

Figure 6 describes radial temperature distributions at $z = 5$. Vertical bars indicate the electron temperature obtained from equation (2) by the previously mentioned Langmuir probe, and the solid curve indicates the thermal equilibrium temperature T estimated from equation (1). As these results agree well with each other, we can conclude the state of the plasma jet at $z = 5$ is nearly at thermal equilibrium; i.e. electron temperature equals heavy-particle tempera-

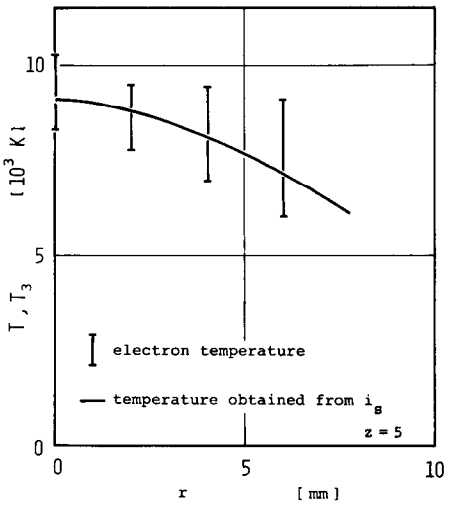

FIG. 6. Radial temperature distributions at $z = 5$.

ture (T_1 and T_2) at $z = 5$. The saturation ion current at $z = 5$ and $r = 0$ is around 2.0×10^4 A m^{-2}.

The results of the heat flow from the rarefied ionized argon to the biased wire are plotted in Fig. 7. At the strongly negative potential region, the heat flow increases linearly, and at the small probe potential region, it increases rapidly. At the region between them, a smoothly varying curve is shown and continues into the above two lines. The solid and dotted lines in this figure are calculated ones which will be explained later.

4. THEORETICAL ANALYSIS AND RESULTS

In the case of the conventional collisionless plasma, the following theoretical investigation can be considered. To get general results, temperatures of constructing species are considered to be different in this section. The probe potential in this investigation is always below the plasma potential.

As a rarefied ionized gas involves ionized species, heat transfer rates depend strongly on them. So, the ionization and kinetic energy increases due to an electric field, and the variations of properties due to the presence of ionized species have to be taken into account as follows. Species in the relevant plasma jet are argon atoms, argon ions and electrons, which are denoted by subscripts 1, 2, and 3, respectively. Therefore, the total heat flux q from the plasma jet to a solid surface may be written as

$$q = q_1 + q_2 + q_3. \tag{3}$$

As the plasma jet is of free molecular flow, heat fluxes due to respective species are written as

$$q_1 = \tfrac{1}{4} n_1 V_1 a_1 (\tfrac{1}{2} m_1 V_1^2 \beta_1 - 2kT_w \gamma_1) \tag{4}$$

$$q_2 = \tfrac{1}{4} n_2 V_2 [a_2 \{\tfrac{1}{2} m_2 V_2^2 \beta_2 - (e\phi + 2kT_w)\gamma_2\} + (u_I - e\phi_w)\gamma_2] \tag{5}$$

and

$$q_3 = \tfrac{1}{4} n_3 V_3 \exp\left(\frac{e\phi}{kT_3}\right)(2kT_3 + e\phi_w) \tag{6}$$

where n_j, V_j, a_j, and m_j are number density, first-order mean molecular velocity, thermal accommodation coefficient, and mass of species j, respectively. T_w is the solid surface temperature, and $2kT_w$ denotes the mean kinetic energy flux of particles at the wall temperature removing from the surface. β_j and γ_j are species j's correction factors for the effect of a flow velocity on the heat fluxes (see Appendix A). Equation (6) does not include the correction factors because the velocity of electrons is so far higher than the flow velocity. The

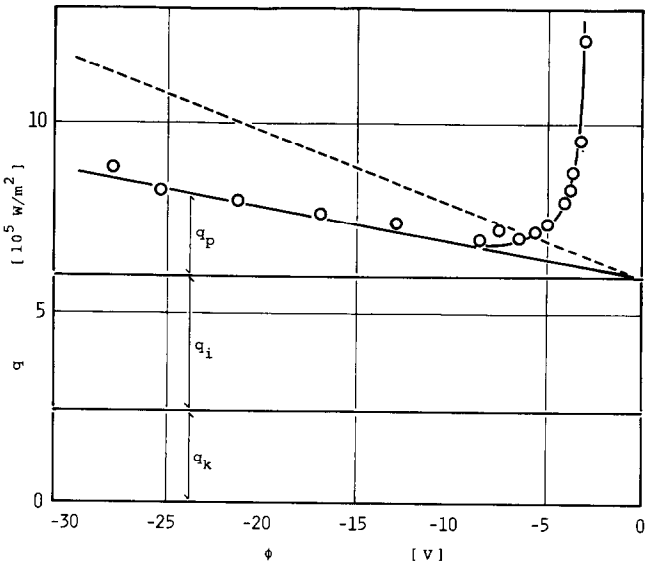

FIG. 7. Heat flow and its theoretical constructions at $z = 5$.

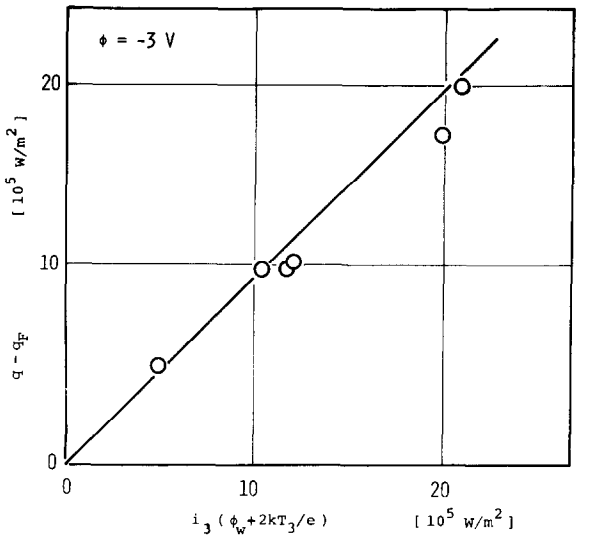

FIG. 8. Heat flow in a small probe potential.

term ϕ denotes the biased probe potential with respect to the plasma potential, and thereby, ϕ is always negative. The term $e\phi$ in equations (5) and (6) denotes the influence of the electric sheath (see Appendix B). Here, all of the ionization energy of ions is assumed to be given to the surface when ions reach the surface. As ions recombine with metal electrons on the surface, they release the energy, the ionization energy minus the energy of work function of the metal, $u_I - e\phi_w$.

In the case of the float potential, equation (3) becomes

$$q = q_F = \tfrac{1}{4}n_1V_1a_1(\tfrac{1}{2}m_1V_1^2\beta_1 - 2kT_w\gamma_1) + \tfrac{1}{4}n_2V_2[a_2\{\tfrac{1}{2}m_2V_2^2\beta_2 - (e\phi_F + 2kT_w)\gamma_2\} + (u_I + 2kT_3)\gamma_2] \quad (7)$$

and the difference between the heat flux at an arbitrary potential and that at the float potential is

$$q - q_F = \tfrac{1}{4}n_2V_2a_2e(\phi_F - \phi)\gamma_2 + \tfrac{1}{4}n_3V_3\left\{\exp\left(\frac{e\phi}{kT_3}\right) - \exp\left(\frac{e\phi_F}{kT_3}\right)\right\} \times (2kT_3 + e\phi_w). \quad (8)$$

In the case of a small probe potential ($\phi \simeq 0$), this reduces to

$$q - q_F = i_3\left(\frac{2kT_3}{e} + \phi_w\right) \quad (9)$$

where

$$i_3 = \tfrac{1}{4}n_3V_3\exp\left(\frac{e\phi}{kT_3}\right)e. \quad (10)$$

This relation is compared with the measured values and shown in Fig. 8. This shows a good agreement and supports the above view.

In the case of a strongly negative potential where the present experiments are mainly carried out, equation (3) becomes

$$q = q_1 + q_2 \quad (11)$$

and by differentiating with respect to the potential

$$\frac{\partial q}{\partial \phi} = \tfrac{1}{4}n_2V_2a_2e\gamma_2 = a_2i_s \quad (12)$$

where the saturation ion current i_s is given by

$$i_s = \tfrac{1}{4}n_2V_2e\gamma_2. \quad (13)$$

From equation (12), the accommodation coefficient of ions, a_2, can be obtained experimentally.

In the above discussion, the heat flow was classified in the view of species, but it can be done in the view of types of energy; i.e. kinetic, ionization and potential energy. Equation (11) also can be written as

$$q = q_k + q_i + q_p, \quad (14)$$

where

$$q_k = \tfrac{1}{4}(n_1a_1 + n_2a_2)V(\tfrac{1}{2}mV^2\beta - 2kT_w\gamma) \quad (15)$$

$$q_i = \tfrac{1}{4}n_2V(u_I - e\phi_w)\gamma \quad (16)$$

and

$$q_p = -\tfrac{1}{4}n_2Va_2e\gamma\phi = -a_2i_s\phi \quad (17)$$

where $T_1 = T_2$, $m_1 = m_2 = m$, $V_1 = V_2 = V$, $\beta_1 = \beta_2 = \beta$ and $\gamma_1 = \gamma_2 = \gamma$. Pressure is given by

$$P = k(n_1T_1 + n_2T_2 + n_3T_3). \quad (18)$$

By using equations (13) and (18), n_1 and n_2 in equation (15) are eliminated, and then

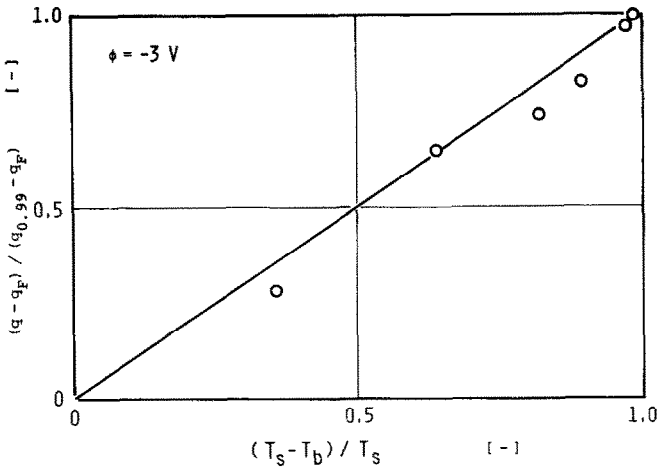

FIG. 9. Checking up of the effect of a break time on a heat flow.

$$q_k = \frac{1}{4}\left[a_1\left\{\frac{P}{kT_1} - \frac{4i_s}{Ve\gamma}\frac{T_1+T_3}{T_1}\right\} + a_2\left(\frac{4i_s}{Ve\gamma}\right)\right]V(\tfrac{1}{2}mV^2\beta - 2kT_w\gamma). \quad (19)$$

In this equation, the unknown factor is only a_1, because T_3 can be obtained from the probe characteristic, T_1 is equal to T_3 as the results of Fig. 6, and a_2 also can be obtained from equation (12), and then the thermal accommodation coefficient of argon atoms can be obtained experimentally.

The results calculated at the strongly negative potential region are shown in Fig. 7. q_k, q_i, and q_p are also indicated in this figure. The broken line indicates the heat flow under the assumption of $a_2 = 1$. According to values of q_p and q_k, the accommodation coefficient of atoms is obtained to be 0.62 by equation (19), and that of ions is 0.48 by equation (12).

5. DISCUSSION

The plasma jet has been considered to be in the free molecular flow, and this condition has to be examined. From the results of Fig. 6, temperature is 9000 K, the saturation ion current is 2.0×10^4 A m^{-2} and thereby ion or electron density is evaluated to be 2.3×10^{20} m^{-3}. Therefore, Debye length is calculated to be 4.4×10^{-7} m and 3×10^{-3} times smaller than the diameter of the wire (1.5×10^{-4} m). On the other hand, the mean free path of argon atoms is estimated to be 3×10^{-3} m, and so, Knudsen number becomes 20. These values support the free molecular flow condition, and suggest the conventional collisionless plasma diagnostics is available. We also investigated the relationship between the diameter of the wire and the heat flux to the wire. The heat fluxes to the wires whose diameter is $\leqslant 3 \times 10^{-4}$ m were shown to be constant. This result also supports the free molecular flow condition.

We also investigated the effect of the break time T_b on the heat flow to the probe. The probe potential was kept at -3 V, the switching frequency was kept at 330 Hz and only the break time was varied. The heat flow from the plasma jet at this potential depended mainly on the electron current, while the heat flow at the float potential was only slightly dependent: this is shown by equations (9) and (7), respectively. Therefore, the difference between the heat flow at -3 V and that at the float potential depends on the electron current, i.e. the potential, directly. Figure 9 shows the relationship between these differences and the break times which are respectively normalized. It indicates that the differences are in direct proportion to $(T_s - T_b)/T_s$. This means that 3% less heat transfer is obtained in this experiment because T_b is 3% of T_s; this error is considered to be negligible. Therefore, the ratio of T_b to T_s seems to be valid to obtain the heat flow.

In this experiment, a bias potential to the probe was given with respect to the anode. However, the transport phenomena of charged species depend on the potential difference ϕ between the plasma and probe potential as used in the present theory. When experimental and theoretical results are compared in Fig. 7, it is necessary to adjust the above mentioned ϕ and bias potential. For the adjustment, the float potential was used because it can be obtained both experimentally and theoretically. Theory indicates the following relation [6]

$$\phi_F = \frac{kT_3}{e}\ln\frac{V_2\gamma_2}{V_3} \quad (20)$$

where ϕ_F denotes the potential difference between the float and plasma potential, and γ_2 denotes the flow velocity correction factor explained at Appendix A. From the above equation, we get $\phi_F = -5$ V.

The temperature rise during the heat flux measure-

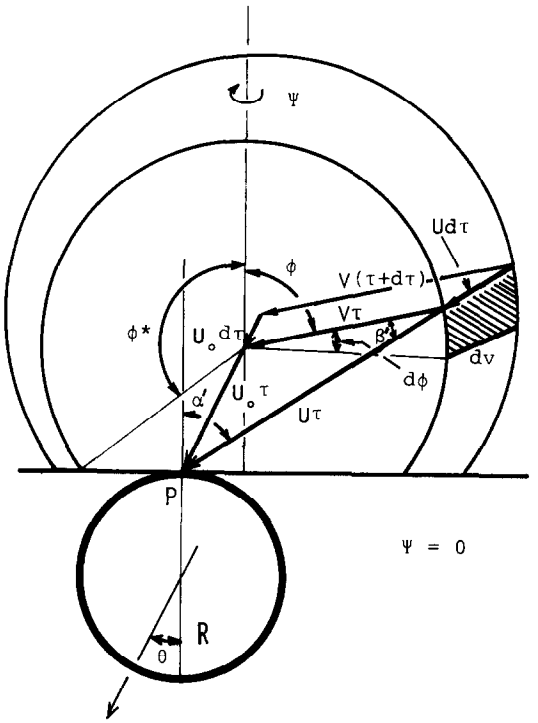

FIG. 10. A model of collisionless heat transfer in a flowing media.

ment is 100 K maximum. On the other hand, the temperature of the gas is about 9000 K. The variation of the wall temperature is 1% of the temperature difference. So, the wall temperature T_w may be given as 300 K.

From Equation (19), the accommodation coefficient of argon atoms is given by

$$a_1 = \frac{8kTq_k}{PmV^3\beta} \tag{21}$$

where $T_1 = T_2 \gg T_w$ and $n_1 \gg n_2$ are assumed. As the variation of β in this experiment is small in comparison with other factors, this equation becomes

$$\ln a_1 = \ln q_k - \ln P - \tfrac{1}{2}\ln T + \text{const.} \tag{22}$$

Similarly,

$$\ln a_2 = \ln q_p - \ln i_s - \ln(-\phi). \tag{23}$$

So, the accuracies of a_1 and a_2 are same order of those of q_k, q_p, P, i_s and $-\phi$, and twice higher of that of T.

6. CONCLUSION

By applying a square wave potential to the probe, it can be possible to measure the heat flow from a rarefied ionized gas to a biased probe, and the electron temperature simultaneously.

The heat flow varies in direct proportion to an applied potential at the strongly negative potential region and increases rapidly in the near zero potential.

Thermal accommodation coefficients of argon atoms and ions can be obtained individually by measuring the heat transfer from the rarefied ionized argon gas flow to a biased solid (tungsten) surface. The thermal accommodation coefficient of argon atoms to a tungsten wire is different from and larger than that of argon ions. The former is 0.62 and the latter is 0.48 in this experimental condition.

REFERENCES

1. M. Smoluchowski, On conduction of heat by rarefied gases, *Phil. Mag.* **46,** 192–206 (1898).
2. M. Knudsen, Die Molikulare Wärmeleitung der Gase und der Akkommodationskoeffizient, *Ann. Physik* **34,** 593–656 (1911).
3. J. K. Roverts, The exchange of energy between gas atoms and solid surfaces, *Proc. R. Soc.* **A129,** 146–161 (1930).
4. F. M. Devienne, *Advances in Heat Transfer*, Vol. 2, p. 271, (edited by J. P. Hartnett and T. F. Irvine, Jr.). Academic Press, New York (1965).
5. G. S. Springer, *Advances in Heat Transfer*, Vol. 7, p. 163, (edited by T. F. Irvine, Jr. and J. P. Hartnett). Academic Press, New York (1971).
6. F. F. Chen, *Plasma Diagnostic Techniques*, (edited by R. H. Huddlestone and S. L. Leonard), Chap. 4. Academic Press, New York (1965).

APPENDIX A

As the flow velocity u_0 at $z = 5$ is estimated to be 1300 m s^{-1} at maximum, and the first mean velocity of argon atoms and ions at 9000 K is 2200 m s^{-1}, the maximum of u_0/V is about 0.6 and the effect of flow velocity on heat flux has to be considered. Therefore, a model as shown in Fig. 10 is considered, and the amounts of heat fluxes are calculated. The figure is the side view of a wire (thick circle, its radius R) in a uniform flow velocity u_0. The point P on the surface of the wire which possesses the position vector **P** is considered. The particles which will reach the point P after time τ will be on the sphere whose center is indicated by $\mathbf{P} - \mathbf{u}_0\tau$ and radius is $V\tau$. The particles which reach the point P between time τ and $\tau + d\tau$ are in the space between the above sphere and a new one whose center is $\mathbf{P} - \mathbf{u}_0(\tau + d\tau)$ and radius is $V(\tau + d\tau)$. The volume element shown in Fig. 10 is integrated over all the possible presenting region with respect to ϕ, ψ, θ. The possible region is the space which is enclosed by the above two spheres and the plane which contacts the wire at the point P, and only the opposite side of the wire. Furthermore, Maxwell–Boltzmann velocity distribution is assumed. Heat flow due to species j per unit length of the wire is given by

$$Q_j = \frac{1}{d\tau}\int_0^1\int_0^{\pi}\int_0^{\infty}\int_0^{\phi^*}\int_0^{\pi} \times E_j n_j f_j(4Rv^2 w \sin\phi\cos\alpha')\,d\psi\,d\phi\,dv\,d\theta\,dl \tag{A1}$$

where E_j = kinetic $(m_jV_j^2/2)$ or ionization energy (u_I). The effects due to flow velocity are dependent upon the type of the energy, i.e. kinetic or ionization. So, we can define two correction factors, β, γ

$$Q_{jk} = 2\pi R(\tfrac{1}{4}n_jV_j)(\tfrac{1}{2}m_jV_j^2)\times\beta \tag{A2}$$

and

$$Q_{ji} = 2\pi R(\tfrac{1}{4}n_jV_j)u_I\times\gamma. \tag{A3}$$

From equations (A1)–(A3), these factors are evaluated as a function of $y\ (= u_0/V_j)$

$$\beta = \frac{\pi}{2}\left(1 + \frac{5}{\pi}y^2 + \frac{2}{\pi^2}y^4\right) \tag{A4}$$

and

$$\gamma = 1 + \frac{2}{\pi} y^2. \tag{A5}$$

These equations are valid in the case of $y < 1$. The errors of above equations are around 5% in the case of $y = 0.6$.

APPENDIX B

Changed particles are accelerated or decelerated by an electric field; namely charged particles which go through an electric sheath gain or lose their kinetic energy. The effect of the presence of the sheath on heat flux due to ions is always positive and that of electrons is negative; i.e. the kinetic energy flux due to ions is represented by the term of $(m_2 v_2^2/2) - e\phi$ and that for electrons is $(m_3 v_3^2/2) + e\phi$, where ϕ denotes the probe potential and thereby ϕ is always negative. Furthermore, not all of the electrons which reach the surface of the sheath can reach the surface of a wall, although ions can. Only the electrons which possess the kinetic energy of $(m_3 v_3^2/2) + e\phi > 0$ can reach. Therefore, the kinetic energy due to ions for $y = 0$ is reduced to

$$q_{2s} = \pi n_2 \left(\frac{m_2}{2\pi k T_2}\right)^{3/2} \int_0^{\infty} \int_0^{\pi/2} (\tfrac{1}{2} m_2 v_2^2 - e\phi) v_2^3 \times \exp\left(-\frac{m_2 v_2^2}{2kT_2}\right) \sin 2\phi \, d\phi \, dv_2$$
$$= \tfrac{1}{4} n_2 V_2 (2kT_2 - e\phi) \tag{A6}$$

and that for electrons is reduced to

$$q_{3s} = \pi n_3 \left(\frac{m_3}{2\pi k T_3}\right)^{3/2} \int_{v^*}^{\infty} \int_0^{\phi} (\tfrac{1}{2} m_3 v_3^2 + e\phi) v_3^3 \times \exp\left(-\frac{m_3 v_3^2}{2kT_3}\right) \sin 2\phi \, d\phi \, dv_3$$
$$= \tfrac{1}{4} n_3 V_3 \exp\left(\frac{e\phi}{kT_3}\right) (2kT_3) \tag{A7}$$

where $m_3(v^*)^2/2 + e\phi = 0$, and $m_3(v_3 \cos \phi^*)^2/2 + e\phi = 0$.

TRANSFERT THERMIQUE ENTRE UN GAZ IONISE RAREFIE ET UN FIL FIN DE TUNGSTENE POLARISE ELECTRIQUEMENT

Résumé—On effectue une étude expérimentale et théorique du transfert thermique entre un jet de plasma d'aigon raréfié, partiellement ionisé (500 Pa, 9000 K) et un fil fin de tungstène polarisé électriquement.

Les flux de chaleur sur le fil sont obtenus à partir des variations de résistance électrique. Lorsque le fil est polarisé la résistance ne peut être mesurée de façon précise parce que le courant à travers le circuit de polarisation perturbe les mesures. Aussi le courant est coupé par un circuit d'interruption pendant un temps court (0,1 ms) toutes les 3 ms pour mesurer la résistance.

La variation de flux thermique avec le potentiel de polarisation peut être obtenue et les coefficients d'accomodation des atomes d'argon et des ions sont déterminés, soit 0,62 pour les atomes d'argon et 0,48 pour les ions d'argon.

WÄRMEÜBERTRAGUNG VON EINEM VERDÜNNTEN IONISIERTEN GAS AN EINEN ELEKTRISCH VORGESPANNTEN FEINEN WOLFRAMDRAHT

Zusammenfassung—Es wurden experimentelle und theoretische Untersuchungen zum Wärmeübergang eines verdünnten, teilweise ionisierten Argonplasmastrahls (500 Pa, 9000 K) an einen elektrisch vorgespannten feinen Wolframdraht gemacht. Die Wärmeströme zum Draht wurden durch die Änderungen seines elektrischen Widerstandes bestimmt. Wenn der Draht unter Vorspannung steht, kann der Widerstand nicht genau gemessen werden, weil der Strom aufgrund der Vorspannung die Messung behindert. Deshalb wird der Strom durch einen Schaltkreis für kurze Zeit (0, 1 ms) alle 3 Millisekunden unterbrochen, um den Widerstand zu messen. Es konnten die Änderung der Wärmeströme mit dem Vorspannungspotential erhalten werden, auch wurden die Anpassungskoeffizienten für Argonatome und-ionen bestimmt, wobei sich 0,62 für Argonatome und 0,48 für Argonionen ergab.

ТЕПЛОПЕРЕНОС ОТ РАЗРЕЖЕННОГО ИОНИЗИРОВАННОГО ГАЗА К ТОНКОЙ ВОЛЬФРАМОВОЙ ПРОВОЛОКЕ, ИМЕЮЩЕЙ ПОТЕНЦИАЛ СМЕЩЕНИЯ

Аннотация — Проведены экспериментальные и теоретические исследования переноса тепла от разреженной частично ионизированной аргоновой плазменной струи (500 Pa, 900 K) к тонкой вольфрамовой проволоке, имеющей потенциал смещения.

Интенсивность переноса тепла к проволоке определялась по изменению ее электрического сопротивления. Если проволока обладает потенциалом смещения, ее сопротивление не поддается точному измерению из-за воздействия тока в цепи смещения. Поэтому для измерения сопротивления ток через каждые 3 миллисекунды отключался на короткое время (0,1 мсек) с помощью переключающей схемы. Получена зависимость интенсивности переноса тепла от потенциала смещающего напряжения и определены коэффициенты аккомодации атомов и ионов аргона: 0,62 для атомов и 0,48 для ионов аргона.